Mon. Not. R. Astron. Soc. **265**, 101–114 (1993)

Neutral hydrogen at high redshifts as a probe of structure formation – I. Post-*COBE* analysis of CDM and HDM models

K. Subramanian[1]★ and T. Padmanabhan[2]†

[1]*National Centre for Radio Astrophysics, TIFR, Poona University Campus, Ganeshkind, Pune 411007, India*
[2]*Inter University Centre for Astronomy and Astrophysics, Poona University Campus, Ganeshkind, Pune 411007, India*

Accepted 1993 May 11. Received 1993 April 5; in original form 1992 November 20

ABSTRACT

The structures that form in the Universe at redshifts $z \lesssim 10$ can be detected and studied using the redshifted 21-cm line emission from neutral hydrogen. We compute the expected comoving number density, N, of protocondensates that will emit a flux higher than S, at various redshifts, in the CDM and HDM models. The models are normalized using *COBE* results. Our results are compared with the present and expected future sensitivities of various telescopes for the detection of protocondensates. In the CDM models the predicted maximum fluxes at a redshift $z \simeq 3.3$ are about (1.5–3) mJy and $N \simeq (10^{-8}$–$10^{-7})$ Mpc^{-3}. These protocondensates cannot be detected with present sensitivities, but will become detectable in the near future with improved sensitivities. At lower redshifts, the detectability of these structures critically depends on their neutral hydrogen content. In the redshift range around $z \simeq 5$, *individual* protocondensates will not be detectable. The excess variance due to fluctuations with small density contrasts will, however, be detectable with somewhat large (say, about 60-h) integration time. At still higher redshifts, it will be virtually impossible to see any signal, even with such a large integration time. Biased CDM models predict larger fluxes, but somewhat lower abundances. Finally, the HDM models – when normalized using *COBE* results – do *not* lead to a detectable number of sources ('pancakes') at redshifts $z \gtrsim 2$.

Key words: galaxies: formation – dark matter – large-scale structure of Universe – radio lines: general.

1 INTRODUCTION

It is generally believed that galaxies and other large-scale structures in the Universe originated by the growth of small initial perturbations via gravitational instability. If this picture is correct, then one should be able to see some signature of the protocondensates in the Universe at a redshift range of, say, $z \lesssim 10$ or so. Sunyaev & Zeldovich (1972, 1974) first pointed out that the birth of the large-scale structures could possibly be probed by observing the (redshifted) 21-cm line emitted by neutral hydrogen in the incipient galaxies and clusters. If such radiation is detected, it could open up an entirely new window to the high-redshift Universe.

Several searches have been made so far at metre wavelengths for the redshifted 21-cm line. Many of these searches yielded only null results (cf. Subrahmanyan & Anantharamaiah 1990; Subrahmanyan & Swarup 1990; Uson, Bagri & Cornwell 1991a; Wieringa, de Bruyn & Katgert 1992, and references cited therein). Recently, however, Uson, Bagri & Cornwell (1991b) have claimed the first-ever detection of a neutral-hydrogen-rich protocluster at $z = 3.4$. The Giant Meterwave Radio Telescope (GMRT) presently being constructed in India – and expected to go into operation by 1994 – should be able to improve the observational situation considerably as regards the detection and study of protocondensates containing neutral hydrogen (Swarup 1984). It is, therefore, interesting to work out the expected flux of redshifted 21-cm emission in various models of structure formation and compare the results with both the present observational limits and the expected sensitivity limits of future instruments such as the GMRT.

The expected properties of 21-cm emission from protoclusters depend sensitively on the theory of galaxy formation. While several authors (Sunyaev & Zeldovich 1974; Hogan & Rees 1979; Subrahmanyan 1989; Scott & Rees 1990;

★ e-mail:kandu@gmrt.ernet.in.
†e-mail:paddy@iucaa.ernet.in.

Subramanian & Swarup 1992) have studied this issue in the past, a comprehensive analysis of the problem, taking into account different models for structure formation, has not yet been carried out. This is the first of a series of papers addressing this question. Here we work out the expected number densities of protocondensates in the cold dark matter (CDM) and hot dark matter (HDM) models. Future papers will address the details of the line profile, the expected pattern of sky brightness and the detailed ionization history of the Universe.

Definitive predictions about the 21-cm emission could not be made in the past because of the following crucial difficulty. Theories of structure formation are usually specified by giving the power spectrum of density fluctuations, up to a normalization constant. Until recently this normalization constant was an unknown parameter, introducing a major ambiguity to the predicted flux of the 21-cm emission. Recently, however, the *COBE* satellite has detected (Smoot et al. 1992) temperature anisotropies of the cosmic microwave background radiation (CMBR). Using the *COBE* results, one can unambiguously fix the normalization constant in the power spectrum of any specific model. This reduces the uncertainty in theoretical models to a great extent, and allows us to perform a more reliable calculation.

This paper is organized as follows. In the next section, we will discuss the possible sources of 21-cm line emission in the Universe, and some details regarding the observational procedures. In Section 3, which forms the core of the paper, we will derive the detailed properties of these sources in the CDM model. These results are presented in terms of the expected number $N(S)$ of sources emitting flux larger than some value S. We calculate $N(S)$ for different redshifts and for a range of values of the parameters in the problem. Section 4 describes why the HDM models do not perform as well as the CDM models when both are normalized properly using the *COBE* results. The last section presents a short summary of the paper.

2 NEUTRAL HYDROGEN AT HIGH REDSHIFTS: SOURCES AND DETECTION

A 21-cm (or, equivalently, a 1420-MHz) photon is emitted when a hydrogen atom makes a transition from a state in which the electron and proton spins are aligned to a state in which the spins are anti-aligned. It is usual to define an effective 'spin' temperature T_s by the relation $n(\text{up})/n(\text{down}) = \exp(-\Delta E/kT_s)$, where $n(\text{up})$ denotes the population of the upper level, $n(\text{down})$ that of the lower level, and ΔE is the energy difference between the levels. The relative magnitude of T_s with respect to the background radiation temperature, T_b, will then decide whether absorption or emission will be the dominant effect in a given cloud of neutral hydrogen; a cloud will be seen in emission if $T_s > T_b$ and in absorption if $T_s < T_b$. Scott & Rees (1990) have examined this issue in detail for several models for structure formation and have concluded that $T_s > T_b$ in most of the situations that are probable. We will also be dealing mostly with cases in which the neutral hydrogen structure shows up in emission.

Further, in all the cases we consider, the optical depth of the hydrogen cloud to the 21-cm photons is quite small. Hence one can calculate the flux in the emission line by adding the photons emitted by each hydrogen atom in the cloud. It can be shown (see e.g. Spitzer 1978) that the peak flux density (S_ν) of the 21-cm line radiation, from an optically thin cloud containing neutral hydrogen of mass $M_{\text{H I}}$, is

$$S_\nu = 5.3\ \text{mJy} \left(\frac{M_{\text{H I}}}{10^{13}\ \text{M}_\odot}\right) \left(\frac{\Delta\nu_0}{1\ \text{MHz}}\right)^{-1} \times \frac{\Omega_0^4 h^2}{\{\Omega_0 z + (\Omega_0 - 2)[(1+\Omega_0 z)^{1/2} - 1]\}^2}. \quad (1)$$

Here $\Delta\nu_0$ is the frequency width (FWHM for a Gaussian profile) of the observed emission line, z is the redshift of the cloud, Ω_0 is the density parameter of the Universe, and h is the Hubble constant in units of 100 km s^{-1} Mpc^{-1}. The frequency width can be related to the velocity width (Δv) of the cloud by $\Delta\nu_0/\nu_0 = \Delta v/c$; that is,

$$\Delta\nu_0 = \frac{4.7}{1+z}\ \text{MHz} \left(\frac{\Delta v}{1000\ \text{km s}^{-1}}\right). \quad (2)$$

Thus the peak flux density (which we shall hereafter call just 'flux') can be computed if the mass of neutral hydrogen and the velocity dispersion are known. As we shall see later, the velocity dispersion can be obtained from the gravitational dynamics of the cloud; the *total* mass of the cloud can also be related to various other known quantities in the problem. The mass of *neutral* hydrogen contained in the cloud needs now to be related to the total mass. To do this, we have to take into account the fact that existing observations of quasars at high redshifts already constrain the neutral hydrogen content of the Universe at $z \lesssim 5$.

First, the absence of any (Gunn–Peterson) dip in the ultraviolet spectra of quasars shortward of the Lyα emission line suggests that any smoothly distributed hydrogen in the Universe is likely to be almost completely ionized at $z \lesssim (4\text{–}5)$ (Gunn & Peterson 1965; Miralda-Escudé & Ostriker 1990). It is, however, possible to regenerate neutral hydrogen from the intergalactic medium (IGM) during gravitational collapse, provided that the gas can cool efficiently. In the hierarchical models for structure formation, this is expected to happen on subgalactic scales first and on progressively larger scales later. (In the HDM model – in which cluster mass scales collapse first to form pancake-like structures – a significant fraction of the hydrogen will become neutral as the gas in the dense pancake cools. This was the major source of neutral hydrogen discussed in the original papers of Sunyaev and Zeldovich. We will see later that this model – unfortunately – fails to produce a detectable signal. The reason for this is connected to the fact that the *COBE* results have now fixed the normalization constant in the spectrum uniquely; see Section 5).

Secondly, although quasar spectra do not show the Gunn–Peterson dip due to smoothly distributed H I, they do exhibit many H I absorption lines, indicating the existence of neutral hydrogen in clumped form. The damped Lyα systems are particularly interesting in the present context (Wolfe et al. 1986; Turnshek et al. 1989; Wolfe 1989; Lanzetta et al. 1991). These absorbers contain, at their observed redshift of $z \sim (2\text{–}4)$, as much mass in neutral hydrogen as the total stellar content of all present-day disc galaxies. In fact, Wieringa et al. (1992) make the interesting

point that the observed abundance of these systems may also be consistent with a scenario in which the bulk of the precursors of rich clusters are still neutral at redshifts of $z \simeq (2\text{–}4)$.

The above considerations suggest that we should focus on the emission from clumps or collections of clumps – revealed by, for example, the absorption lines in quasar spectra – if we want to detect H I at $z \lesssim 5$. This will be of relevance in what follows.

In the following sections we shall consider different models of galaxy formation and work out the expected flux of line emission from neutral hydrogen at several redshifts. While these results can be computed – in principle – for any redshift, it is certainly more useful to concentrate on the redshifts that are being directly probed by existing and future instruments. One of the frequency bands that is currently being used by several groups is the band around 327 MHz, corresponding to a redshift of $(1420/327)-1=3.34$. A significant part of this paper is devoted to working out the expected line emission from sources at this redshift. The GMRT will also be able to probe several other frequency bands around 610, 233 and 150 MHz, corresponding to redshifts of 1.33, 5.1 and 8.47 respectively. We shall also examine the expected 21-cm flux from these epochs.

The actual search for 21-cm flux generally proceeds in the following manner. One uses a Fourier-synthesis telescope consisting of both a compact array of antennas and an extended array. The extended array is used to make a high-resolution image of the continuum emission over the field of view. This is then subtracted from the data acquired by the compact array, leaving behind the line emission in the presence of noise. The resulting data can be smoothed to various angular ($\Delta\theta$) and frequency ($\Delta\nu$) resolutions to produce a spectral line data cube. (There will, of course, be a minimum $\Delta\theta$ defined by the synthesized beamsize, θ_s, and a minimum frequency resolution that can be attained by a given telescope.) The spectral-line cube samples a comoving volume of space whose two dimensions are defined by the area covered by the primary beam and whose depth is proportional to the total frequency bandwidth. The cube itself is made up of pixels defined by $\Delta\theta$ and $\Delta\nu$. The choice of $\Delta\theta$ is governed by the desire to maximize the signal-to-noise ratio. If one chooses too small a $\Delta\theta$, then only part of the source will be observed in each pixel and the signal will be small. On the other hand, if $\Delta\theta$ is taken to be so large that there are few antenna pairs with correspondingly small baselines, the noise will increase. Hence, ideally, the instrumental resolution has to match the angular size of the protocluster. Similarly, $\Delta\nu$ is chosen so that the noise is minimized and at the same time the emission line spans a width of at least $\Delta\nu$.

The spectral-line cube can be analysed in two different ways to see if there are signals of 21-cm emission. First, one can look for correlated pixels that have much higher levels of flux than the rms noise (σ_N) per pixel. Typically, one would look for pixels with a peak flux greater than $5\sigma_N$ above the noise. Secondly, one can investigate whether there is an excess variance in the flux per pixel, over and above the noise. The first strategy is useful for detecting isolated luminous objects, while the second method may be useful in picking out an inhomogeneous (but not highly overdense) distribution of neutral hydrogen. We shall mostly deal with the predictions for the first type of signal, and will comment on the second approach whenever relevant. The main question, therefore, is the following. Given a detection system (such as, say, GMRT) operating at a set of frequency bands and some model for structure formation, what is the abundance of objects emitting a flux higher than, say, n times the rms noise level of the instrument? We shall now take up this issue, beginning with the cold dark matter (CDM) model for structure formation.

3 THE 21-cm FLUX IN THE CDM MODEL

3.1 Preliminary considerations

In the CDM model for galaxy formation, the Universe is dominated by dark matter particles with negligible random velocities. It is usual to assume that the primordial density field is a random Gaussian variable with a power spectrum of the Harrison–Zeldovich form: $P(k)=Ak$. The power spectrum at sufficiently late epochs – say, just after recombination – is well approximated by the fitting function

$$P(k)=\frac{Ak}{(1+Bk+Ck^{3/2}+Dk^2)^2} \tag{3}$$

(Peebles 1983; Davis et al. 1985), with $B=1.7(\Omega_0 h^2)^{-1}$ Mpc, $C=9(\Omega_0 h^2)^{-3/2}$ Mpc$^{3/2}$ and $D=1(\Omega_0 h^2)^{-2}$ Mpc^2. The shape of the power spectrum is completely specified by the dynamics, while the amplitude A can now be fixed by comparing the quadrupole anisotropy in the microwave background radiation (MBR) produced by this spectrum with the observed *COBE* result. Such an analysis (see e.g. Padmanabhan & Narasimha 1992) gives a value of $A=[(24\pm4)\ h^{-1}\ \text{Mpc}]^4$. We shall use the value $A=(24\ h^{-1}\ \text{Mpc})^4$ unless otherwise stated.

The mean-square fluctuation $\sigma^2(R)=\langle(\delta M/M)^2_R\rangle$ in the mass contrast within a sphere of radius R, placed randomly somewhere in the Universe, can be related to $P(k)$ by

$$\sigma^2(R)=\int_0^\infty \frac{\mathrm{d}k}{k}\left[\frac{k^3P(k)}{2\pi^2}\right]\left[\frac{3(\sin kR-kR\cos kR)}{(kR)^3}\right]^2. \tag{4}$$

We show in Fig. 1 a plot of $\sigma(R)$ for the CDM power spectrum, linearly extrapolated to the present epoch, adopting the *COBE* normalization. One sees that $\sigma(R)$ is fairly flat at small subgalactic scales, decreases gently with R and falls off asymptotically as $\sigma\simeq(R_0/R)^2$ with $R_0\simeq24\ h^{-1}$ Mpc. Since $\sigma(R)$ is a (gently) decreasing function of R, small mass scales will collapse first in this model. Structures will form hierarchically, with larger mass scales going non-linear at later times. Since a sphere of comoving radius R will contain a mean mass of $M(R)=(4\pi/3)\rho_0R^3$ (where ρ_0 is the mass density of the Universe at present), we can also treat σ as a function of the mass scale: $\sigma(M)=\sigma[R(M)]$. In what follows, we shall use either form depending on which is more convenient.

The functions $P(k)$, $\sigma(R)$ and $\sigma(M)$ can always be approximated locally by a power law: if $P(k)\propto k^n$, then $\sigma\propto R^{-(n+3)/2}\propto M^{-(n+3)/6}$; the effective index n is (-3) at small scales and increases to 1 at large scales. At $M\simeq10^9$ M$_\odot$, $n=-2.3$; at $M\simeq10^{12}$ M$_\odot$, $n=-2$; and at $M\simeq10^{15}$ M$_\odot$, $n=-1$.

Given $\sigma(M)$, one can estimate the redshift $z_{\rm coll}$ at which a mass scale M collapses and forms a bound object. Consider,

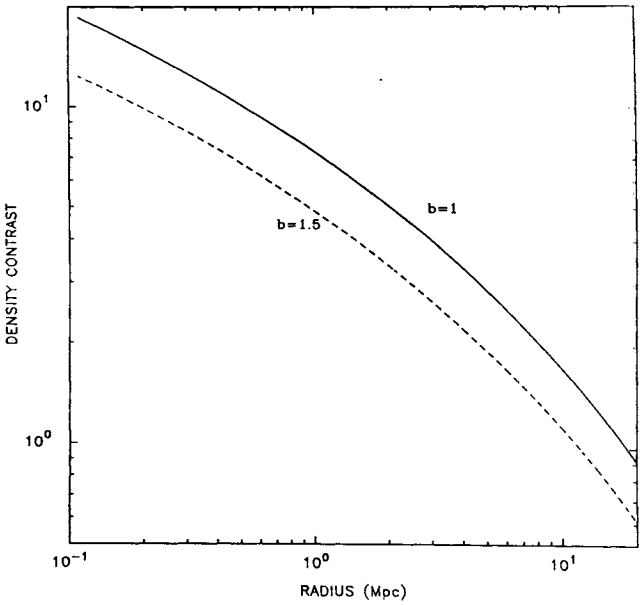

Figure 1. A plot of $\sigma(R)$ versus R for the CDM models with the bias parameters $b=1$ (solid line) and 1.5 (dashed line).

for example, a spherical region of radius R containing a density contrast $\delta_0(R)$ which is n times the variance $\sigma(R)$ at that scale. The standard spherical model (see e.g. Peebles 1980) then leads to an estimate

$$(1+z_{\rm coll})=\frac{\delta_0(R)}{1.686}=\frac{n\sigma(R)}{1.686}. \tag{5}$$

(We stress the convention that $\delta_0(R)$ is the average excess density contrast in a sphere of radius R, linearly extrapolated to the present epoch.) With the *COBE* normalization, typical (i.e. 1σ) regions containing cluster scale masses (10^{14} $M_\odot$) collapse only at low redshifts, $z\simeq 0.35$; even a 4σ fluctuation on cluster scales [which has a relative probability of $\exp(-8)\simeq 3.35\times 10^{-4}$] collapses only at $z\simeq 4.4$. At the redshifts probed by various H I searches, therefore, protoclusters could *not* have collapsed and virialized in the CDM models. (We shall see in Section 5 that the situation is worse for HDM models.) From the constraints discussed in the previous section, it follows that gas that is *smoothly distributed* within the protocluster will *not* be neutral for $z\lesssim 5$.

There is, however, another source of neutral hydrogen in these models (e.g. Subramanian & Swarup 1992). Note that, in the CDM picture, smaller mass scales do have a large enough σ for them to collapse at high redshifts; hence the gas that has collapsed into these small mass scale objects could cool and form neutral clumps of hydrogen. A region of the size of a protocluster will then consist of many small-scale clumps containing neutral hydrogen, provided that the ionization processes are not effective. The photons constituting the metagalactic UV flux and the UV photons emitted during the formation of massive stars could play a possible role in ionizing the gas in these clumps. The metagalactic flux is so efficient at heating the gas in small clumps ($M\lesssim 10^9$ $M_\odot$) that these clumps do not collapse in the first place (e.g. Efstathiou 1992). For larger masses, however, such heating cannot prevent the collapse of the gas. In this case, the gas in the clumps becomes dense enough to prevent significant ionization by the metagalactic UV photons. As far as star formation is concerned, the degree of ionization depends crucially on the rate of star formation Q. Unfortunately, Q is not known with any degree of precision. One can, however, put some limits on Q, at least in the case of the damped Lyα systems; these limits suggest that Q cannot be so large as to ionize the gas in a young galaxy significantly, at least as long as it has not converted the bulk of its gas into stars (Cowie 1988; Subramanian & Swarup 1992). Assuming that the clumps we are considering are similar in structure to the damped Lyα systems seen at high redshifts, we could expect the gas to be neutral at these redshifts in spite of star formation. These clumps can be a significant source of the 21-cm flux from such a protocluster. We shall now estimate this flux.

3.2 Flux from the clumps in a protocondensate

To calculate the flux we have first to estimate the fraction of gas in a protocluster that is in the form of collapsed objects ($f_{\rm coll}$), at any particular redshift. Of this, a further fraction, say $f_{\rm N}$, will be in the form of H I. Suppose that $f(M, z)\,{\rm d}M$ is the number density of collapsed objects at a redshift z within a mass range of M to $M+{\rm d}M$. Let us assume that the gas in a collapsed object can cool efficiently if it has a mass in the range $M_1<M<M_2$. From the usual cooling arguments applied to the CDM model (cf. Blumenthal et al. 1984; Efstathiou 1992), one can estimate that $M_1\simeq 10^9$ $M_\odot$ and $M_2\simeq 10^{12}$ $M_\odot$. Hence the mass of H I contained in the small-scale objects populating a protocluster of proper volume V and excess density contrast $\delta(z)$ is

$$M_{\rm H\,I}=f_{\rm N}f_{\rm b}\int_{M_1}^{M_2} Mf(M,z)\,{\rm d}M\times V\times[1+\delta(z)], \tag{6}$$

where $f_{\rm b}$ is the fraction of the mass in the Universe that is in the form of baryons. In practice, we will take V to be the volume of a sphere of radius l, where l is related to the angular resolution $\Delta\theta$ of the telescope by the equation

$$\Delta\theta=l(1+z)^2\frac{H_0}{2c}\frac{\Omega_0^2}{\Omega_0 z+(\Omega_0-2)[(1+\Omega_0 z)^{1/2}-1]}$$
$$\approx 0.57\ \text{arcmin}\ h\frac{1+z}{1-(1+z)^{-1/2}}\left(\frac{l}{1\ \text{Mpc}}\right),\qquad \text{for } \Omega_0=1. \tag{7}$$

(This is the standard relation between the proper length at redshift z and the angle it subtends at the observer.)

An estimate of $f(M, z)$ can be obtained from the hierarchical clustering theory of Press & Schechter (1974). Using the Press–Schechter formula for the mass function of collapsed objects, we obtain

$$\int_{M_1}^{M_2} Mf(M,z)\,{\rm d}M=-\int_{M_1}^{M_2} M\left[\frac{\bar\rho}{M}\left(\frac{{\rm d}F}{{\rm d}M}\right)\right]{\rm d}M$$
$$=\bar\rho(z)[F(M_1)-F(M_2)]=\bar\rho(z)\,f_{\rm coll}(z), \tag{8}$$

where

$$F=\text{erfc}\left[\frac{\delta_{\rm c}(t,t_i)}{\sqrt{2}\sigma(R,t_i)}\right]=\text{erfc}\left[\frac{1}{\sqrt{2}}\left(\frac{M}{M_{nl}}\right)^{(3+n)/6}\right]. \tag{9}$$

In the above equation, $\delta_c(t, t_i)$ is the critical excess density contrast needed at time t_i so that the fluctuation collapses at time t; $\sigma(R, t_i) = \sigma(R)/(1+z_i)$, and erfc is the complementary error function defined by

$$\mathrm{erfc}\,(x) = \frac{2}{\sqrt{\pi}} \int_x^\infty \mathrm{d}t \exp(-t^2). \tag{10}$$

In arriving at the last equality in equation (9), we have used the (local) power-law approximation $P(k) \propto k^n$, and expressed the results in terms of the mass scale $M_{nl}(z)$ that is collapsing at redshift z. This mass can be estimated from the spherical model by solving the (implicit) equation $\sigma[R(M_{nl})] = 1.686(1+z)$, where $R(M) = (3M/4\pi\rho_0)^{1/3}$ and ρ_0 is the cosmological density at present. (For example, the redshift 3.34 corresponds to $M_{nl} \approx 3 \times 10^{11}\,\mathrm{M}_\odot$; the values of M_{nl} for several relevant redshifts are given in Table 1; b is the bias parameter, to be discussed in Section 3.4.)

Note that $f(M, z)$ has a maximum at a value $M_{\max}(z)$, which increases as z decreases. Since we are computing the collapsed fraction (which can cool effectively) by using a fixed window in mass (M_1, M_2), we find that $f_{\rm coll}$ increases, reaches a maximum, and then decreases as z decreases. In reality, when objects of mass $M \simeq M_2$ merge to form a larger mass their H I may not be completely destroyed, especially if the baryons have sunk to the centre of the potential well. Hence the $f_{\rm coll}$ calculated above could be an underestimate. Note also that the Press–Schechter formula does not take into account the possible influence of a background large-scale overdensity on $f(M, z)$. This point is discussed in detail in the Appendix. It turns out that this effect is subdominant to the inherent uncertainties in the values of $f_{\rm N}, f_{\rm b}$ and $f_{\rm coll}$.

Writing the volume V as $(4\pi/3)l^3$ (where l is a *proper* radius), we can express the neutral hydrogen mass as

$$\begin{aligned} M_{\rm H\,I} &= \overline{M}_{\rm H\,I} \times [1+\delta(z)] \\ &= f_{\rm N} f_{\rm b} f_{\rm coll}(z) \rho_0 (1+z)^3 \times \frac{4\pi}{3} l^3 \times [1+\delta(z)] \\ &\approx 0.73 \times 10^{13}\,\mathrm{M}_\odot\, h_{50}^2 \Omega_0 \left(\frac{f_{\rm N}}{0.5}\right)\left(\frac{f_{\rm b}}{0.1}\right)\left(\frac{f_{\rm coll}}{0.5}\right) \\ &\quad \times \left[\frac{l(1+z)}{10\ \mathrm{Mpc}}\right]^3 [1+\delta(z)] \end{aligned} \tag{11}$$

where $h_{50} = (h/0.5)$. Substituting (2) and (11) in (1), we find that

$$\begin{aligned} S_{\rm exp} &= 0.202\ \mathrm{mJy}\, \frac{h_{50}^4}{g(z)} \left(\frac{f_{\rm N}}{0.5}\right)\left(\frac{f_{\rm b}}{0.1}\right)\left(\frac{f_{\rm coll}(z)}{0.5}\right) \\ &\quad \times \left[\frac{l(1+z)}{10\ \mathrm{Mpc}}\right]^3 \left(\frac{\Delta v}{1000\ \mathrm{km\ s^{-1}}}\right)^{-1} (1+\delta), \end{aligned} \tag{12}$$

where Δv is the velocity width of the protocluster, $g(z) = (1+z)[1-(1+z)^{-1/2}]^2$ and we have set $\Omega_0 = 1$.

There is, however, one further complication that needs to be accounted for. This expression gives the flux from a region with density $\overline{\rho}(1+\delta)$ and velocity Δv. The uniform background will, of course, contribute an amount proportional to $(\overline{\rho}/\Delta v_{\rm H})$, where $\Delta v_{\rm H}$ is the velocity width due to the Hubble expansion across the radius of the protocluster. Since the observations look for a signal above the background, one has to subtract out the H I emission from the regions surrounding the protocluster. Hence the expected *signal* is proportional to

$$S_{\rm sig} \propto \left[\frac{\overline{\rho}(1+\delta)}{\Delta v} - \frac{\overline{\rho}}{\Delta v_{\rm H}}\right] \propto \left[\frac{\overline{\rho}(1+\delta)}{\Delta v}\right] f_{\rm sig}, \tag{13}$$

where the factor $f_{\rm sig} = 1 - (\Delta v)/[\Delta v_{\rm H}(1+\delta)]$ takes into account the difference between the signal and background. Thus the final expression for the flux is

$$S_{\rm sig} = S_{\rm exp} \times f_{\rm sig}. \tag{14}$$

The above subtlety makes very little difference to the actual results when we have $1+\delta \gg 1$ and $\Delta v \ll \Delta v_{\rm H}$, because in this case $f_{\rm sig} \approx 1$. If, however, we are considering high redshifts at which $\delta \ll 1$, then we have to take account of the factor $f_{\rm sig}$. In this linear regime of density contrast, we have $\Delta v \approx \Delta v_{\rm H}(1-\delta/3)$ and $f_{\rm sig} \approx 4\delta/3$.

Some of the scalings used in (14) deserve comment. Arguments based on big bang nucleosynthesis suggest that the baryonic fraction of the Universe is about 0.1 (for $h = 0.5$), which is the value we have adopted. The fraction $f_{\rm N}$ of these baryons, which are in the form of neutral hydrogen, is somewhat uncertain and its precise estimate requires detailed consideration of the thermal, ionization and star formation histories of the gaseous component during the formation of the structures. This is a subject of interest in its own right, and we plan to address it in a future publication. In this work, we shall be content to take this number to be of order unity. This estimate should be valid at least for high redshifts, say $z \gtrsim 3$. A direct motivation for this assumption comes from the observations of the damped Lyα systems discussed in the previous section, which show that the H I detected in these systems is comparable to the stellar content of all present-day galaxies.

The other unknown quantities in (14) can all be estimated from the power spectrum [or $\sigma(R)$] and by invoking a model for non-linear evolution. We shall use here the spherical model to estimate the effects of non-linear evolution. In this model, the density contrast $\delta(z)$ and velocity $v(z)$ at redshift z are given by the (implicit) relations

$$1+\delta(z) = \frac{9}{2}\frac{(\theta - \sin\theta)^2}{(1-\cos\theta)^3}, \tag{15}$$

Table 1. The non-linear masses and collapsed fractions at various z.

redshift	b=1.0		b=1.5	
z	M_{nl}	f_{coll}	M_{nl}	f_{coll}
1.33	$8.6 \times 10^{12} M_\odot$	0.2354	$1.04 \times 10^{12} M_\odot$	0.3388
3.34	$2.9 \times 10^{11} M_\odot$	0.3822	$2.3 \times 10^{10} M_\odot$	0.4283
5.1	$3.4 \times 10^{10} M_\odot$	0.4265	$2.0 \times 10^{9} M_\odot$	0.3531
8.47	$1.3 \times 10^{9} M_\odot$	0.327	–	–

$$1+z=\delta_0\left(\frac{5}{3}\right)\left(\frac{4}{3}\right)^{2/3}(\theta-\sin\theta)^{-2/3}, \tag{16}$$

$$v=\frac{2}{5}\left(\frac{5}{3}\right)^{3/2}\left(\frac{R}{t_0}\right)\delta_0^{1/2}\frac{\sin\theta}{1-\cos\theta}$$

$$\approx 645.5\ \mathrm{km\ s^{-1}}\ \delta_0^{1/2}\ h_{50}\left(\frac{R}{10\ \mathrm{Mpc}}\right)\frac{\sin\theta}{1-\cos\theta}. \tag{17}$$

Here R is the *comoving* radius of the spherically overdense region, which is related to the proper radius l by mass conservation: $R=l[1+\delta(z)]^{1/3}$. The quantity δ_0 is related to the initial density contrast δ_i of the spherical region at some very early epoch z_i by

$$\delta_0=(3/5)\,\delta_i(1+z_i). \tag{18}$$

In other words, δ_0 is the overdensity that the spherical region will have if the linear theory is valid throughout the evolution. Equations (15) and (17) express δ and v in terms of the parameter θ (called the 'evolution angle'), which is related to the redshift by (16). It is often convenient to rewrite (16) as

$$\delta_0=0.4953(1+z)(\theta-\sin\theta)^{2/3}, \tag{19}$$

so that δ_0 is expressed in terms of the evolution angle and the redshift. Notice that the spherical model is parametrized by δ_0 and R.

The velocity width of the line Δv (defined as the FWHM in velocity space) will depend on the density profile of the protocluster. For our purpose, it is sufficient to approximate the density as constant within l. The velocities of shells at different radii r then depend linearly on r; in this case one can easily show that $\Delta v=\sqrt{2}v$. (For a centrally peaked density profile, Δv is probably smaller than the above estimate.) Using equations (14), (15) and (17) and substituting for Δv and $1+\delta(z)$ in terms of θ, we then obtain for the flux

$$S=A(l,z)\left|\left[\frac{\theta-\sin\theta}{\sin\theta(1-\cos\theta)}\right]\right|, \tag{20}$$

where

$$A(l,z)=0.857\ \mathrm{mJy}\ h_{50}^3\left(\frac{f_N}{0.5}\right)\left(\frac{f_b}{0.1}\right)\left(\frac{f_{coll}(z)}{0.5}\right)$$
$$\times\left[\frac{l(1+z)}{10\ \mathrm{Mpc}}\right]^2 f_{sig}\frac{(1+z)^{1/2}}{[1+z-\sqrt{(1+z)}]^2}. \tag{21}$$

The peak flux depends on z, l and the evolution angle θ, which describes how far the protocluster has evolved towards collapse.

Note that, if $\delta\ll 1$, we can calculate the flux directly from the linear theory. In this case, we have

$$\Delta v=\sqrt{2}v_H\left(1-\frac{1}{3}\delta\right)$$

$$\approx 707\ \mathrm{km\ s^{-1}}\ h_{50}(1+z)^{1/2}\left[\frac{l(1+z)}{10\ \mathrm{Mpc}}\right], \tag{22}$$

where we have included a factor $\sqrt{2}$ in calculating the linewidth and set $f_{sig}=4\delta/3$. Using these relations in (14), we obtain

$$S=1.524\ \mathrm{mJy}\ h_{50}^3\ f_N\left(\frac{f_b}{0.1}\right)f_{coll}$$
$$\times\left[\frac{l(1+z)}{10\ \mathrm{Mpc}}\right]^2\frac{\delta(z)}{(1+z)^{1/2}g(z)}. \tag{23}$$

In our expression (20), the flux can increase to very high values if the velocity width Δv tends to zero. The following point, however, should be noted. The smaller scale structures in the protocluster (whose neutral hydrogen is contributing to our flux) will themselves have a velocity width, say $\Delta v_g\simeq 300$ km s^{-1} for 'galactic' mass clumps. Even when the velocity dispersion of the large system falls below that of the constituents, the actual velocity width will therefore still be dominated by that of the constituents. That is, when $\Delta v\lesssim\Delta v_g$ for the protocluster, we must set $\Delta v\simeq\Delta v_g$. We shall need this result later.

Consider now any observational project that is searching for the 21-cm line emission. The details of the instrumental configuration will specify for us the values of l and z. [The value of l corresponds generally to the synthesized beamsize θ_s that is employed in the observations (for which the sensitivity to H I emission is maximized), although we will consider here a range of l about this value.] Once the redshift has been specified, it is straightforward to calculate $M_{nl}(z)$ and to use (9) to estimate f_{coll}. In Table 1 we have also given the f_{coll} estimated for a number of redshifts relevant to present and planned H I observations. All the quantities in equation (21) are now known except θ, which is uniquely related to δ_0 once z is fixed (see equation 19). Given the value of δ_0 we can compute S.

In the standard CDM model, δ_0 is a Gaussian random variable with zero mean and a variance of $\sigma(R)$. Thus the probability that δ_0 has a particular value in the range $[\delta_0,\ \delta_0+\mathrm{d}\delta_0]$ is given by

$$P(\delta_0,R)\,\mathrm{d}\delta_0=\frac{1}{\sqrt{2\pi}\sigma(R)}\exp\left[-\frac{\delta_0^2}{2\sigma(R)^2}\right]\mathrm{d}\delta_0. \tag{24}$$

This probability distribution in δ will translate to the probability $\mathscr{P}(S)\,\mathrm{d}S$ of obtaining a given flux through (14). Integrating this expression from S to infinity, we can find the cumulative probability $Q(S)$ for the flux to be larger than a value S. The *comoving* number density of protocondensates with fluxes larger than S will then be

$$N(S)=Q(S)\left(\frac{4\pi}{3}l^3\right)^{-1}(1+z)^{-3}$$

$$\approx 2.39\times10^{-4}\,Q(S)\left[\frac{l(1+z)}{10\ \mathrm{Mpc}}\right]^{-3}\ \mathrm{Mpc^{-3}}. \tag{25}$$

We can now calculate the expected flux from protoclusters in the CDM model at various redshifts and for a range of radii l, and present the results as N versus S relations. Before we embark on this calculation (which is now straightforward), however, it is worthwhile to study equation (20) closely and to identify the range of values of θ that give a significant flux.

In order to calculate $Q(S)$ for a specified z and l, we have first to find the range of θ that gives a peak 21-cm flux greater than S. The quantity (S/A) is plotted as a function of

θ in Fig. 2. From this figure it is clear that, in general, two different ranges of θ satisfy this condition: a range of $[\theta_1, \theta_2]$ about the value $\theta=\pi$, and a range $[\theta_3, 2\pi]$ with $\theta_2<\theta_3$. (For values of S/A below a certain limiting value, equation 20 has only one root; in which case, the relevant range is $\theta_1<\theta<2\pi$; see below.) The first range corresponds to the case in which the protocluster is sufficiently near the epoch of turn-around ($\theta=\pi$) that the velocity width becomes small, leading to a large flux. The second range corresponds to the case in which the density of the protocluster is tending to infinity because the structure is collapsing to zero radius. This, of course, is an artefact of the spherical model; in reality, the protocluster is likely to virialize and heat up (destroying the neutral hydrogen) long before this epoch. The values of θ greater than some critical value, say θ_c, are therefore unlikely to be of relevance in the physical context. We take $\theta_c=3\pi/2$, which corresponds to the epoch at which the protocluster has collapsed to half its maximum radius. Hence we need to concentrate only on values of θ less than θ_c.

While evaluating the contribution from near the epoch of turn-around, we have to take into account the complication mentioned earlier, namely that the smaller scale structures will themselves have a velocity width, say Δv_g. Even when Δv for the protocluster is very low (i.e. when $\Delta v \lesssim \Delta v_g$), the actual velocity width will therefore still be about Δv_g. This leads to a lower limit on the velocity – and thus an upper limit on the flux S – near turn-around for each z and l.

Given a range of values of θ that contribute a flux greater than S, we can find the corresponding range of δ_0, using (19). The probability $Q(S)$ of finding a flux greater than S can therefore be estimated by simply integrating (24) over the range of δ_0 corresponding to the ranges $\theta_1<\theta<\theta_2$ and $\theta_3<\theta<3\pi/2$. In performing this integration, we should take into account the fact that the comoving radius R also depends on $\delta(z)$ – and hence on θ – via the relation $R=l(1+z)[1+\delta(z)]^{1/3}$. We also adopt an effective power-law approximation for $\sigma(R)=\sigma(R_0)(R_0/R)^m$, where $R_0=(9\pi^2/16)^{1/3}l(1+z)=1.77\,l(1+z)$ is the comoving radius of a protocluster that has a proper radius l at turn-around. We then have

$$Q(S)=\int_{\mathscr{R}}\frac{1}{\sqrt{2\pi}\sigma(R)}\exp\left[-\frac{\delta_0^2}{2\sigma(R)^2}\right]\mathrm{d}\delta_0$$
$$=\frac{2Y}{3\sqrt{2\pi}}\int_{\mathscr{R}}\mathrm{d}\theta(1-\cos\theta)^{1-m}(\theta-\sin\theta)^{(2m-1)/3}$$
$$\times\exp\left[-\frac{Y^2}{2}\frac{(\theta-\sin\theta)^{4(1+m)/3}}{(1-\cos\theta)^{2m}}\right], \qquad (26)$$

where

$$Y=\frac{0.4953(1+z)2^m}{\pi^{2m/3}\sigma(R_0)} \qquad (27)$$

and the range of integration $\mathscr{R}$ is as described above. We can estimate $N(S)$ by substituting (26) in (25).

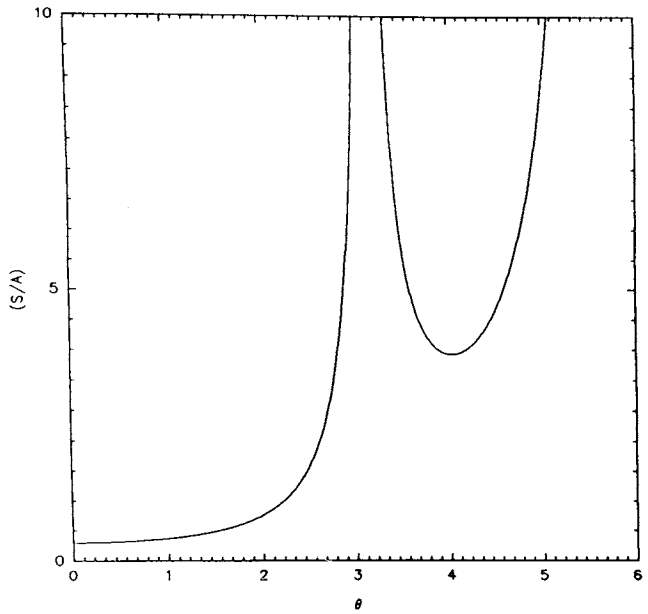

Figure 2. A plot of S/A versus θ.

3.3 Results and discussion

We shall now discuss the results of this computation, and compare it with the present and future sensitivities of various searches. For this, it is advisable first to clarify the actual numbers involved in such observational programmes, in particular the GMRT.

We summarize in Table 2 the numerical values of some of the relevant parameters of the GMRT. (These have been worked out from the data in Swarup et al. 1991, and represent the theoretical expectations based on the design of the GMRT.) Note that the GMRT will have an array of 30 antennas, 14 being configured as a central compact random array in an area of 1 km^2, and the remainder being placed in three arms extending up to 14 km from the centre. We have given in Table 2 the following parameters: (1) the frequencies at which the GMRT will search for redshifted H I; (2) the corresponding redshift that is being probed; (3) the field of view at various frequencies; (4) the angular resolution of the synthesized beam, θ_s, when only the central compact array of antennas is used; (5) the expected rms (thermal) noise limits on the synthesized image for a point source being probed with 100-kHz velocity resolution and 10-h integration by the central array; (6) the comoving volume $\mathscr{V}$ of the Universe sampled per field, assuming a bandwidth of 16 MHz; this is

Table 2. Parameters for H I searches by the GMRT.

Frequency (MHz)	610	327	233	150
Redshift	1.33	3.34	5.1	8.47
Field of view (deg)	0.9	1.8	2.5	3.8
Resolution (arc min)	1.7	3.2	4.5	7.0
rms noise (mJy)	0.24	0.27	0.46	1.25
$\mathscr{V}$ (in 10^6 Mpc^3)	0.44	5.4	11.8	60.0
l(1+z) (Mpc)	2.06	5.84	9.4	16.58

defined by the relation

$$\mathscr{V} = d_A^2 \, d\Omega \, \frac{c \, dt}{dz} \, dz = \frac{4c^3}{H^3} \frac{(\sqrt{1+z}-1)^2}{(1+z)^{5/2}} \, d\Omega \, dz, \tag{28}$$

where d_A is the angular diameter distance and we have set $\Omega_0 = 1$; and (7) the quantity $l(1+z)$, where l is the proper radius of the cloud that subtends the angle θ_s at the observer. These quantities are related by equation (7).

Since the results depend sensitively on redshift, it is preferable to discuss each redshift separately. We begin with the redshift $z = 3.34$, at which most of the present-day searches for 21-cm emission are carried out. For this redshift, the GMRT will have a resolution of about 3.2 arcmin, corresponding to $l(1+z) \simeq 5.84$ Mpc and an expected rms noise $\sigma_N \simeq 0.27$ mJy (Table 2). In searches that have already been carried out with the Westerbork Synthesis Radio Telescope (WSRT) (Wieringa et al. 1992) and with the VLA (Uson et al. 1991a,b), the rms noise level is about 5 times larger for similar resolutions in angular size and frequency. From Table 1 we find that the collapsed fraction at this redshift is $f_{coll} = 0.3822$. We adopt $f_N = 0.5$ for the fraction of gas that is neutral in the collapsed objects and take $\Delta v_g = 300$ km^{-1}, typical of 'galactic' scale clumps.

In Fig. 3(a) we give a plot of $N(S)$ against S for these parameters and for three values of $l(1+z) = 6$, 8, 10 Mpc. For these values of l the masses enclosed by a sphere of

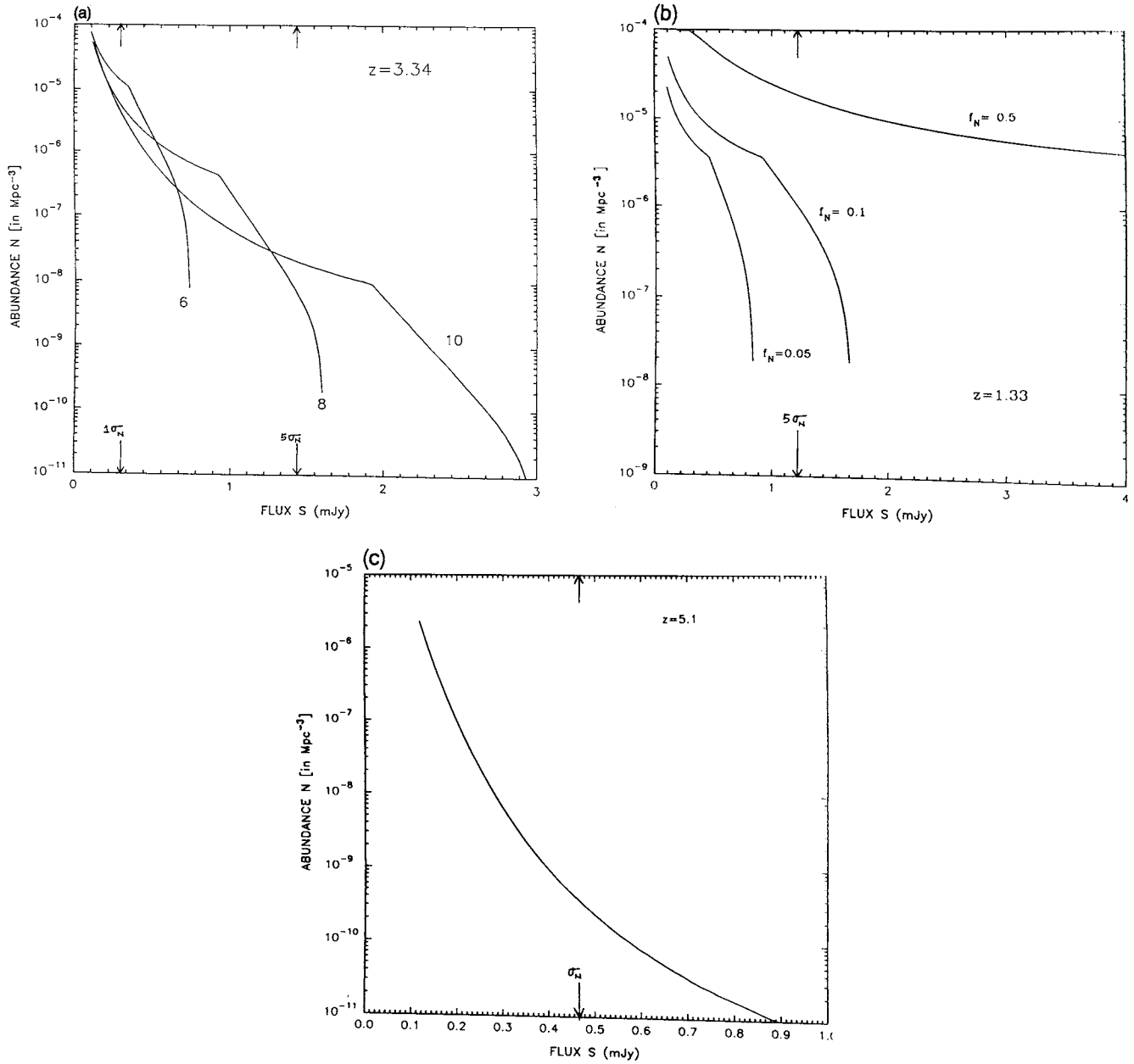

Figure 3. (a) The abundance $N(S)$ of protoclusters with a flux greater than S at $z = 3.34$ for $l(1+z) = 10$, 8 and 6 Mpc. We also mark the $1\sigma_N$ and $5\sigma_N$ noise levels for detection by the GMRT. (b) $N(S)$ versus S at $z = 1.33$ for $f_N = 0.05$, 0.1 and 0.5. We also mark the $5\sigma_N$ noise level for detection by the GMRT. (c) $N(S)$ versus S at $z = 5.1$ for $l(1+z) = 10$ Mpc and $f_N = 0.5$. We also mark the rms noise level for detection by the GMRT.

comoving radius R_0 are 3.5×10^{14} $M_\odot$, 8.3×10^{14} $M_\odot$ and 1.6×10^{15} $M_\odot$ respectively, and the corresponding values of $\sigma(R_0)$ are 1.64, 1.27 and 1.03. The maximum flux that is obtained ranges from 0.7 mJy for $l(1+z)=6$ Mpc to 2.97 mJy for $l(1+z)=10$ Mpc. In this figure we also show for comparison the expected rms noise level, σ_N, for the GMRT at this redshift (for 3.2-arcmin resolution) and also the $5\sigma_N$ level. (Note that there is an abrupt change in the nature of the $N(S)$ curve at some critical flux S_{cr}, with $N(S)$ dropping much more rapidly for $S>S_{cr}$. This is because for $S<S_{cr}$ the range of integration $\mathscr{R}$ is $[\theta_1, 3\pi/2]$, while for $S>S_{cr}$, $\mathscr{R}$ changes to the ranges $[\theta_1, \theta_2; \theta_3, 3\pi/2]$; the contribution from the latter range declines sharply with S.)

The flux in a pixel has to be above 1.4 mJy to be detectable at the $5\sigma_N$ level when a resolution of 3.2-arcmin is used. For this resolution, the maximum flux obtained by our computation is below this value. One can, however, obtain higher fluxes for higher values of l. . The abundance of objects that have a flux above 1.4 mJy is 1.3×10^{-8} Mpc^{-3} for $l(1+z)=8$ Mpc and 2.3×10^{-8} Mpc^{-3} for $l(1+z)=10$ Mpc. (These numbers should be compared with the abundance of rich Abell clusters, which is about 5×10^{-7} h_{50}^3 Mpc^{-3}.) One should also note that each field observed by the GMRT at this redshift will sample a comoving volume of about 5.4×10^6 h_{50}^{-3} Mpc^3. *Hence it should be possible to detect these protoclusters with reasonable integration times and frequency resolutions after scanning about eight fields with the GMRT, provided that the noise level does not increase drastically for a somewhat larger smoothing radius.*

Given the maximum fluxes estimated above and the rms noise levels of the instruments now in operation, it is not surprising that the searches carried out so far have only yielded null results. For the lone reported detection of a protocluster by Uson et al. (1991b), the observed velocity width is $\Delta v\simeq180$ km s^{-1} and the flux is about 11 mJy. For this Δv and $l(1+z)=10$ Mpc, the maximum flux is only about 4.6 mJy, making it difficult to explain the detection of this object in the unbiased CDM models. (We will see in Sections 3.4 and 4 that such an object is also unlikely to exist in the biased CDM or HDM models.)

Now consider the other redshifts that will be probed by the GMRT. At $z=1.33$, the GMRT synthesized beam corresponds to $l(1+z)=2.1$ Mpc. The collapsed fraction is $f_{coll}=0.2354$ from Table 1. It turns out that this radius contains too little mass to give a detectable signal above the noise. To explore the dependence on l, we have also tried a larger value of $l(1+z)=10$ Mpc, which contains a cluster-sized mass. Further, there is considerable uncertainty in the neutral fraction at this redshift, since in CDM models with the *COBE* normalization a significant amount of the gas in the collapsed objects may have already turned into stars by this redshift. To handle this uncertainty, we have considered a range of f_N from 0.05 to 0.5. In Fig. 3(b) we give $N(S)$ versus S plots for $z=1.33$, adopting the above values of l and f_{coll}, for the three values of $f_N=0.05$, 0.1 and 0.5. The maximum fluxes that are obtained for these three values of f_N are 0.83, 1.66 and 8.32 mJy respectively. The abundance of objects expected above, say, 1.5 mJy ranges from 2.1×10^{-7} Mpc^{-3} for $f_N=0.1$ to 1.4×10^{-5} Mpc^{-3} for $f_N=0.5$. (Note that, for the parameters specified in Table 2, the $5\sigma_N$ level is about 1.2 mJy. The rms noise level may, however, be larger for the larger value of l adopted above.) In any case, it appears from the above numbers and Fig. 3(b) that observations at this redshift should place interesting limits on the nature of protoclusters.

At redshifts of 5.1 and 8.47 – which could also be probed by future observations – detectable protoclusters turn out to be extremely rare. For example, at $z=5.1$, adopting $l(1+z)=10$ Mpc, $f_N=0.5$ and $f_{coll}=0.4265$, we find that the maximum flux is 1.75 mJy, whereas the $5\sigma_N$ level for detection by the GMRT is a flux of about 2.3 mJy. We show in Fig. 3(c) a plot of $N(S)$ versus S for this case. Even objects that have fluxes just above the rms noise level of about 0.46 mJy have abundance $N(S)\simeq3.8\times10^{-10}$ Mpc^{-3} for the above parameters.

One may wonder whether the more typical fluctuations with small density contrasts may be detectable at these redshifts due to the excess variance that they may contribute to the flux per pixel. (This is the second method of analysis mentioned in Section 2.) Using (23), we find that the flux from the 1σ density fluctuations at $z=5.1$ and with $l(1+z)=10$ Mpc is about 0.05 mJy. The expected rms noise from Table 2 for a bandwidth corresponding to the Hubble velocity (which is relevant for small density contrasts; see equation 22) and an integration time of 10 h is about 0.12 mJy. Excess variance will therefore exceed the noise if the integration time is about 60 h.

At $z=8.47$, however, for $l(1+z)=16.58$ Mpc (which corresponds to the synthesized beamsize at this z) the excess variance will only be about 0.02 mJy, compared to the corresponding rms noise of 0.30 mJy. CDM models with the *COBE* normalization will therefore be very difficult to probe at these redshifts.

It should be clear from the figures that $N(S)$ declines rather sharply for $S>S_{cr}$. This has the effect that $N(S)$ can change significantly for somewhat small changes in the σ_N of the instrument. Note also that we have calculated σ_N assuming a bandwidth of 100 kHz. On the other hand, the bandwidth corresponding to the minimum velocity width of $\Delta v_g\simeq300$ km s^{-1} will be (2–3) times larger. It may be possible to use this fact to reduce σ_N in the search.

In all the above results, it turns out that detectable flux from protoclusters arises only when the protocluster is near turn-around or when it has collapsed substantially. Further, the latter case (corresponding to $\theta_3<\theta<3\pi/2$) contributes negligibly to $Q(S)$ compared to the former case in which the protocluster is near turn-around. Using this fact, one can obtain a good analytical approximation to the numerical results presented above for the maximum detectable flux. [An analytical estimate of $Q(S)$ is, however, not correspondingly useful because of the presence of the exponential in the expression for $Q(S)$; this makes the answer depend sensitively on the nature of the approximation employed.] Near the turn-around, we can write $\theta=\pi+\varepsilon$, with $(\varepsilon/\pi)\ll1$. To the leading order in ε, (20) becomes

$$S=A(l,z)\left|\frac{\pi}{2\varepsilon}\right|. \tag{29}$$

The velocity width, to the same order, is

$$\Delta v=833\ \text{km s}^{-1}\,\varepsilon h_{50}\left[\frac{l(1+z)}{10\ \text{Mpc}}\right](1+z)^{1/2}. \tag{30}$$

The maximum flux is obtained for the minimum velocity width that corresponds to the condition $|\Delta v| \leq \Delta v_g$ evaluated at equality. This condition translates to

$$|\varepsilon| \leq \frac{0.36}{(1+z)^{1/2}} h_{50}^{-1} \left[\frac{l(1+z)}{10\ \mathrm{Mpc}}\right]^{-1} \left(\frac{\Delta v_g}{300\ \mathrm{km\ s^{-1}}}\right), \quad (31)$$

where we have adopted a typical galactic value of $\Delta v_g \sim 300$ km s^{-1}. The maximum possible flux for given z and l is obtained by setting $\Delta v = \Delta v_g$. We then find that

$$S_{\max} = 4.36\, A(l,z)(1+z)^{1/2} h_{50} \left[\frac{l(1+z)}{10\ \mathrm{Mpc}}\right] \left(\frac{\Delta v_g}{300\ \mathrm{km\ s^{-1}}}\right)^{-1}$$
$$= \frac{3.739\ \mathrm{mJy}}{g(z)} h_{50}^4 \left(\frac{f_N}{0.5}\right) \left(\frac{f_b}{0.1}\right) \left(\frac{f_{\mathrm{coll}}(z)}{0.5}\right)$$
$$\times \left[\frac{l(1+z)}{10\ \mathrm{Mpc}}\right]^3 f_{\mathrm{sig}} \left(\frac{\Delta v_g}{300\ \mathrm{km\ s^{-1}}}\right)^{-1}. \quad (32)$$

From the above equation, adopting $l(1+z) = 10$ Mpc, $f_N = 0.5$ and f_{coll} as in Table 1, we can estimate $S_{\max}$ at various redshifts. We obtain $S_{\max} = 6.35$, 2.44, 1.48 and 0.56 mJy at redshifts 1.33, 3.34, 5.1 and 8.47 respectively. This compares reasonably with the numerical results discussed above.

3.4 Biased CDM models

We now briefly comment on the implications of possible biasing in CDM models, for the expected abundances and fluxes of protoclusters. In the first place, it must be stressed that the most natural interpretation of the *COBE* data would point to an unbiased model, at least at large scales. However, in models with power-law-type inflation, in which gravitational waves can significantly contribute to the CMBR fluctuations, the level of density fluctuations indicated by the *COBE* quadrupole may be smaller than the value adopted above. In this case, $\sigma(R)$ at $R = 8\ h^{-1}$ Mpc may be less than unity, allowing one to make the *COBE* results consistent with biased CDM models. The error bars on the CMBR quadrupole also allow a biasing factor of up to $b \sim 1.5$, even when there is negligible contribution from gravitational waves. For these reasons (and for the sake of completeness), we shall examine the results for the 21-cm emission in the biased CDM models.

The introduction of the bias factor, $b = (\delta\rho/\rho)/(\delta j/j)$, where ρ and j are the mass and luminosity densities respectively on large scales, leads to two effects that are relevant for the computation of abundances and fluxes. First, with a bias parameter b greater than unity, $\sigma(R)$ is reduced by a factor b compared to the unbiased case. Each mass scale therefore collapses at a later stage, and protoclusters that are about to become non-linear are even rarer than the estimates made above (cf. equation 26). There is, however, in principle an important trade-off that is relevant for the detectability of protoclusters; namely, that an enhanced number of small-scale objects may form (per unit mass) in protocluster-type environments compared to the general field. This in turn may lead to the H I content of the protocluster being enhanced by a factor, say, E relative to that estimated in equation (11). Obviously, this will enhance the flux by E. We need to take account of both these effects.

To incorporate the first effect we have to replace $\sigma(R_0)$ in (26) by $[\sigma(R_0)/b]$ and also recompute the values of f_{coll} for the reduced σ. This is easily done. To incorporate the second effect, we need to estimate E, which is more difficult. In order to estimate E one may use both theoretical ideas (Kaiser 1985) and observations of present-day clusters. Bardeen et al. (1986) examined this question in some detail for the biased, $\Omega_0 = 1$, CDM model. For this model, they numerically estimated the degree of enhancement of the galactic number density within a typical Abell cluster forming now, compared to the general field. They assumed $b = 2.5$ and obtained a value of $E \simeq (3\text{–}10)$ depending on how they smoothed the density field (see their table 1). The observed properties of rich clusters can also be used to estimate E (e.g. Dekel & Rees 1987). Suppose that the number of galaxies per unit mass forming in a protocluster is indeed enhanced by a factor E compared to the field. Then, when the cluster collapses (and if the galaxies do not sink to the cluster centre), the excess density contrast in galaxies ($\delta N/N$) will also be a factor E larger than the mass contrast ($\delta M/M$). So

$$E = \frac{\delta N/N}{\delta M/M} = \left(\frac{N_g}{n_b V_a}\right) \left(\frac{M_{\mathrm{cl}}}{\rho_b V_a}\right)^{-1} = \frac{N_g \langle L\rangle}{M_{\mathrm{cl}}} \frac{\rho_c}{n_b \langle L\rangle}$$
$$= \frac{(M/L)_{\mathrm{critical}}}{(M/L)_{\mathrm{cluster}}} \Omega_0. \quad (33)$$

Here N_g is the number of galaxies in a cluster of volume V_a and mass M_{cl}, n_b is the average galaxy number density in the field, and ρ_b is the background density of the Universe. Also, in (33) we have multiplied and divided by the average luminosity of a cluster galaxy $\langle L\rangle$. Taking $(M/L)_{\mathrm{cluster}} \simeq (200\text{–}400)\ h\ (\mathrm{M_\odot/L_\odot})$ and $(M/L)_{\mathrm{critical}} \simeq 1500\ h\ (\mathrm{M_\odot/L_\odot})$ (Efstathiou, Ellis & Peterson 1988), we obtain $E \simeq (3.75\text{–}7.5)\Omega_0$. At a more fundamental level, it may be noted that the observation $(M/L)_{\mathrm{critical}} > (M/L)_{\mathrm{cluster}}$ needs to be explained in any theoretical model for structure formation. Biasing at large scales offers one possible explanation.

It is interesting to point out at this stage that arbitrarily large values of E cannot result from biasing. Recall that one may estimate the fraction of the mass in collapsed objects from Press–Schechter theory. Biasing can at most enhance this fraction to a value of unity. E is therefore constrained to a value such that $Ef_{\mathrm{coll}} \lesssim 1$. We also give in Table 1 the f_{coll} estimated from Press–Schechter theory for $b = 1.5$. One can see that E is constrained by $E \lesssim (2\text{–}3)$. We will return to this interesting constraint in a later work.

Adopting a value for $b = 1.5$ and a value of E such that $Ef_{\mathrm{coll}} = 1$, we have recomputed the expected $N(S)$. This is shown in Fig. 4 for the case $z = 3.34$ and $l(1+z) = 8$ Mpc; we have also shown for comparison the corresponding unbiased case. In the biased case the number of expected objects with a flux $S \gtrsim 1.4$ mJy is $\sim 1.5 \times 10^{-8}$ Mpc^{-3}, for $l(1+z) = 8$ Mpc. This is similar to the abundance obtained in the unbiased case. The decrease in probability due to $b > 1$ has therefore been virtually cancelled out by the increase in the effective collapsed fraction Ef_{col}.

In the biased case, one can obtain – in principle – much larger fluxes. For example, fluxes greater than 10 mJy can be obtained with $Ef_{\mathrm{coll}} = 1$ if we take $l(1+z) = 10$ Mpc, $f_N = 0.5$ and a minimum $\Delta v = 180$ km s^{-1} as the relevant parameters

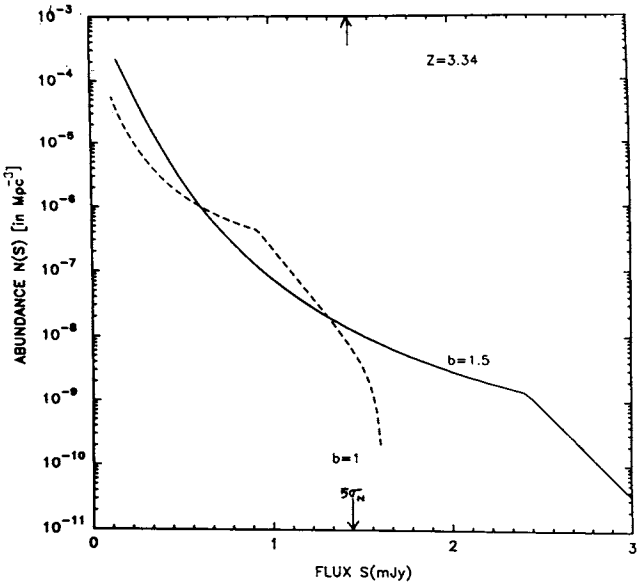

Figure 4. $N(S)$ versus S for a biased CDM model with $b=1.5$ at $z=3.34$. We adopt $l(1+z)=8$ Mpc, and also show the corresponding unbiased case for comparison. The $5\sigma_N$ noise level for detection by the GMRT is marked.

for the object reported by Uson et al. (1991b). *However, this feature is more than offset by the fact that the number density of objects with fluxes greater than this value turns out to be negligibly small:* ranging from $N\simeq 10^{-14}$ Mpc^{-3} for $b=1.5$ to $N\simeq 10^{-12}$ Mpc^{-3} for $b=1.3$. Even with biasing, it is therefore highly unlikely that we will detect objects with such large fluxes.

4 THE 21-cm FLUX IN THE HDM MODEL

A dark matter particle that is still relativistic when it decouples is called hot dark matter. In these models, the large free-streaming velocity wipes out the fluctuations on small mass scales and the processed spectrum has maximum power at cluster scales. Massive protoclusters are the first structures to collapse in this scenario. This collapse is expected to occur preferentially along one axis, leading first to pancake-like structures; the gas in the pancakes cools and later fragments to form galaxies. In this model, each cluster is supposed to have gone through a phase in which the gas is in the form of a cooled neutral hydrogen pancake. It is these pancakes that one would like to detect by their 21-cm emission.

A typical example of a HDM candidate is a massive neutrino with a mass of $m_\nu\simeq 91.5\Omega_\nu h^2$ eV, where Ω_ν is the density of neutrinos in units of the critical density. For $\Omega_\nu=1$ and $h=0.5$, the neutrino mass is constrained to be $m_\nu\lesssim 25$ eV. (Note that, for the $\Omega=1$ model that we are considering, h is constrained to be less than about 0.6.) In the HDM models the power per logarithmic interval in k is given by

$$\Delta^2(k)=\frac{k^3P(k)}{2\pi^2}=\frac{Ak^4}{2\pi^2}\exp[-4.61(k/k_{\rm FS})^{3/2}] \qquad (34)$$

(cf. Bond & Szalay 1983), where $k_{\rm FS}=0.16$ Mpc^{-1} $(m/30$ eV), and A is a normalization constant. From the *COBE* quadrupole data we can determine the value of the normalization constant to be $A=(24\,h^{-1})^4$ Mpc^4 as before. From (34) we can calculate the scale, say $k_{\rm m}$, for which the power in density fluctuations has a maximum. This is the scale that will collapse first, at a redshift that depends on the magnitude of $\Delta(k)$ at $k_{\rm m}$. A simple calculation gives $k_{\rm m}=0.69\,k_{\rm FS}$, corresponding to a mass scale $M_{\rm c}\simeq 3.76\times 10^{14}\,h_{50}^2\,{\rm M}_\odot$ and

$$\Delta_{\rm max}=\Delta(k_{\rm m})=1.4\left(\frac{h}{0.5}\right)^{-2}\left(\frac{m_\nu}{25\ {\rm eV}}\right). \qquad (35)$$

Note that the *COBE* results (which fix A) have completely eliminated any uncertainty in this value. We have seen earlier that the collapse of structures occurs when the linear density contrast (extrapolated to the present) is of order unity. Using the spherical model for non-linear evolution, we have from (5) that

$$(1+z_{\rm coll})\approx\frac{n\Delta_{\rm max}}{1.68}=0.83\,nh_{50}^{-2}\left(\frac{m_\nu}{25\ {\rm eV}}\right) \qquad (36)$$

for an $n\sigma$ fluctuation, even at the scale that has the maximum power. The *COBE* normalization therefore implies that the first structures in the HDM theory will typically begin to go non-linear only at the present epoch. *This, in turn, implies that the high-redshift cluster-scale pancakes of H I that are being looked for in the searches will be quite rare in the HDM model.* The expected comoving number density $N_{\rm p}$ of such objects, at any redshift z, can be easily estimated. The Gaussian statistics for the linear density field imply that the abundances of structures of mass scale $M_{\rm c}$ will be

$$N_{\rm p}\simeq\frac{\rho_0}{M_{\rm c}}\exp\left(-\frac{n^2}{2}\right)$$
$$\approx 1.86\times 10^{-4}\,h_{50}^2\,{\rm Mpc}^{-3}\exp[-0.73(1+z)^2\,h_{50}^4\,m_{25}^{-2}]. \qquad (37)$$

From (37) we have $N_{\rm p}\simeq 3.5\times 10^{-6}$ Mpc^{-3} at $z=1.33$ and $N_{\rm p}\simeq 2.15\times 10^{-10}$ Mpc^{-3} at $z=3.34$. Except at the low redshift of $z=1.33$, the detection of such pancakes will therefore be an extremely rare event in protocluster searches, if HDM theories are correct.

Note that in the earlier versions of HDM models the normalization constant could be arbitrarily chosen so as to have a sufficient number of pancakes collapsing at high redshifts in order to explain high-z quasars and galaxies. With the advent of the *COBE* results, however, one no longer has the freedom to choose a larger value for A. It should also be added here that any gravitational wave contribution to the CMBR fluctuations detected by *COBE* will further reduce the probability for collapse of pancakes at high z. One sees here the extent to which *COBE* has proved useful in constraining HDM models, and, indirectly, the expected 21-cm signals. This is a significant departure from the pre-*COBE* days when HDM models were considered the main provider of neutral hydrogen pancakes at high redshifts.

The flux from a pancake with mass $M_{\rm c}$ and a neutral fraction $f_{\rm N}=0.5$ is about 1.9 mJy $(\Delta v/1000$ km s$^{-1})^{-1}$ at $z=1.33$ and about 0.44 mJy $(\Delta v/1000$ km s$^{-1})^{-1}$ at $z=3.34$.

The expected flux from a pancake may not therefore pose as serious a problem for detectability as the expected abundance of pancakes at high redshifts. Also note that, at $z = 5.1$, the excess variance in the flux per pixel is about 0.08 mJy, which is comparable to the corresponding value in the CDM model and hence will be detectable with sufficiently long integration time. The fact that the first collapsed structures in HDM models form only at low z, however, renders the HDM model itself very unattractive as a theory of structure formation.

The following point needs to be stressed. In the above argument, we have applied the result of a spherical model to the peak scale without explicitly taking into account the effects of asymmetry in protocluster collapse. Due to asymmetric collapse, the short axis of the protocluster could turn around at high redshift, while the long axis does so only at low z. It might seem at first that this fact might help one to violate the above bound: could it be that the long axis collapses only at low z but the pancake collapses along the short axis at higher z, due to asymmetry in the initial density field? This effect, however, cannot play any significant role when the peak power is low. Notice that the density in a typical region of the Universe will increase to non-linear values if the pancake formation (due to the collapse along the short axis) takes place at a significant rate. This, in turn, will increase the rms power at the corresponding scales to values far higher than unity. Hence significant production of pancakes cannot occur as long as the rms power at all scales remains less than the critical value, $\delta_c = 1.68 \simeq 1$. In other words, collapse along the short axis as well as the production of a significant amount of pancakes can take place only *after* the peak scale has gone non-linear. The above calculation shows that this occurs at a very low redshift.

For the sake of completeness, it may be mentioned that we have also analysed mixed models in which both HDM and CDM candidates are present. They do not provide any improvement over the CDM models studied in Section 3 as regards the flux or abundance.

5 SUMMARY

In this paper we have been concerned with the predictions from the CDM and HDM models for the detectability of protocondensates using redshifted 21-cm emission. For this purpose we have calculated the expected fluxes and abundances of protocondensates in these models for a number of redshifts. These results have been compared with the capabilities of various present and planned searches for neutral hydrogen.

It was generally believed in the past that the most promising sources of H I are cluster-size objects that have collapsed into pancakes. These are thought to occur naturally in HDM models; however, the *COBE* results, by fixing the normalization of the power spectrum, have ruled out this possibility at $z \gtrsim 2$.

Cluster-mass objects also collapse at a low redshift in the CDM models. However, there exists another source of H I in these models which results from the collapse and cooling of gas into smaller mass clumps at sufficiently high redshifts. Previous studies of the detectability of H I condensates in CDM models have tended to neglect this feature. The present work shows that protoclusters consisting of smaller mass H I clumps may be detectable in sufficient numbers (about 10^{-8} Mpc^{-3}) and with large enough fluxes (1.5–3 mJy) at redshifts $z \simeq 3.3$. The planned searches with the GMRT, for example, are likely to detect these objects with reasonable integration times. At lower redshifts ($z \simeq 1.3$), the major uncertainty is the fraction of the collapsed gas that remains as H I. If this fraction is about 0.1, one should be able to detect protoclusters at a flux level of 1.5 mJy and an abundance of about 10^{-7} Mpc^{-3}. In the redshift range around $z \simeq 5$, *individual* protocondensates will not be detectable. The excess variance due to fluctuations with small density contrasts will, however, be detectable with somewhat large (say, about 60 h) integration time. At still higher redshifts, it would be virtually impossible to see any signal, even with such a large integration time. [This is in agreement with the results obtained by Scott & Rees (1990) at $z = 8$.]

We have also looked at the possible effect of biasing in the CDM model. In this case the predicted fluxes are larger but the abundance at any flux level depends sensitively on the value of the bias parameter b.

The object reported by Uson et al. (1991b) at $z = 3.4$, with a flux of about 10 mJy, is extremely unlikely to arise in *any* of the models. It cannot be a Zeldovich pancake, since the predicted abundance of such pancakes is about 10^{-10} Mpc^{-3} in the HDM models normalized using *COBE* results. It is rare in CDM models as well for the following reason. To explain the high flux of this object one needs an enhanced fraction of collapsed objects in the protocluster and hence a biasing in the model. This, however, makes the expected abundance very small, ranging from 10^{-12} Mpc^{-3} for $b = 1.3$ to 10^{-14} Mpc^{-3} for $b = 1.5$. If the detection of this object is confirmed it could pose a serious problem for all models.

The major uncertainty in our work arises from the lack of knowledge of the ionization and the thermal history of the gaseous component. We plan to return to this question in a later publication.

ACKNOWLEDGMENTS

We thank Pramesh Rao, C. R. Subrahmanya, Ravi Subrahmanyan and Govind Swarup for helpful conversations. We also thank a referee for bringing to our attention the work of Bower and its relevance to the present problem.

REFERENCES

Bardeen J. M., Bond J. R., Kaiser N., Szalay A. S., 1986, ApJ, 304, 15
Blumenthal G. R., Faber S. M., Primack J. R., Rees M. J., 1984, Nat, 341, 517
Bond J. R., Szalay A. S., 1983, ApJ, 274, 443
Bower R. G., 1991, MNRAS, 248, 332
Cowie L. L., 1988, in Kaiser N., Lasenby A. N., eds, The Post Recombination Universe. Kluwer, Dordrecht, p. 1
Davis M., Efstathiou G., Frenk C. S., White S. D. M., 1985, ApJ, 292, 371
Dekel A., Rees M. J., 1987, Nat, 326, 455
Efstathiou G., 1992, MNRAS, 256, 43P
Efstathiou G., Ellis R. S., Peterson B. A., 1988, MNRAS, 232, 431
Gunn J. E., Peterson B. A., 1965, ApJ, 142, 1633
Hogan C. J., Rees M. J., 1979, MNRAS, 188, 791
Kaiser N., 1985, ApJ, 284, L9

Lanzetta K. M., Wolfe A. M., Turnshek D. A., Lu L., McMahon R. G., Hazard C., 1991, ApJS, 77, 1
Miralda-Escudé J., Ostriker J. P., 1990, ApJ, 350, 1
Padmanabhan T., Narasimha D., 1992, MNRAS, 259, 41P
Peebles P. J. E., 1980, Large Scale Structure of the Universe. Princeton Univ. Press, Princeton, NJ
Peebles P. J. E., 1983, ApJ, 263, L1
Press W. H., Schechter P., 1974, ApJ, 187, 425
Scott D., Rees M. J., 1990, MNRAS, 247, 510
Smoot G. F. et al., 1992, ApJ, 396, L1
Spitzer L., 1978, Physical Processes in the Interstellar Medium. Wiley–Interscience, New York
Subrahmanyan R., 1989, PhD thesis, Indian Institute of Science, Bangalore
Subrahmanyan R., Anantharamaiah K. R., 1990, JA&A, 11, 221
Subrahmanyan R., Swarup G., 1990, JA&A, 11, 237
Subramanian K., Swarup G., 1992, Nat, 359, 512
Sunyaev R. A., Zeldovich Ya. B., 1972, A&A, 20, 189
Sunyaev R. A., Zeldovich Ya. B., 1974, MNRAS, 171, 375
Swarup G., 1984, Giant Metre-Wavelength Radio Telescope – Proposal. Radio Astronomy Centre, TIFR, India
Swarup G., Ananthakrishnan S., Kapahi V. K., Rao A. P., Subrahmanya C. R., Kulkarni V. K., 1991, Curr. Sci., 60, 95
Turnshek D. A., Wolfe A. M., Lanzetta K. M., Briggs F. H., Cohen R. D., Foltz C. B., Smith H. E., Wilkes B. J., 1989, ApJ, 344, 567
Uson J. M., Bagri D. S., Cornwell T. J., 1991a, ApJ, 377, L85
Uson J. M., Bagri D. S., Cornwell T. J., 1991b, Phys. Rev. Lett., 67, 3328
Wieringa M. H., de Bruyn A. G., Katgert P., 1992, A&A, 256, 331
Wolfe A. M., 1989, in Frenk C. S., Ellis R. S., Shanks T., Heavens A. F., Peacock J. A., eds, The Epoch of Galaxy Formation. Kluwer, Dordrecht, p. 101
Wolfe A. M., Turnshek D. A., Smith H. E., Cohen R. D., 1986, ApJS, 61, 249

APPENDIX

The 21-cm emission we have computed arises from neutral clumps of gas residing in a protocondensate. Such a protocondensate is likely to have a density larger than that of a typical region of the Universe. In fact, we obtain a fairly large flux from the condensate when it is near turn-around. In computing the mass function $f(M, z)$ – and $f_{\rm coll}$ – in the text, we have not taken into account the fact that the collapsed objects are not located in a typical region of the Universe but in a region that already has an overdensity. We now estimate $f_{\rm coll}$ taking this effect into account. It turns out that our results are not changed significantly.

To include this effect, it is necessary to obtain the conditional multiplicity function $f[M, \delta_{\rm c}(z)|M', \delta']\,{\rm d}M$, which gives the number density of the objects of mass M that will have collapsed by redshift z when the background region has a mass M' and a density contrast δ'. This has been studied by Bower (1991), to whose paper we refer the interested reader for details. Using the results of Bower it is straightforward to compute $f_{\rm coll}$; we find that equations (8) and (9) in the text are replaced by

$$\int_{M_1}^{M_2} Mf(M, z)\,{\rm d}M = -\int_{M_1}^{M_2} M\left[\frac{\bar{\rho}}{M}\left(\frac{{\rm d}F}{{\rm d}M}\right)\right]{\rm d}M$$

$$= \bar{\rho}(z)[F(M_1) - F(M_2)] = \bar{\rho}(z)\, f_{\rm coll}(z), \quad \text{(A1)}$$

where

$$F = {\rm erfc}\left\{\frac{[\delta_{\rm c}(t, t_i) - \delta_{\rm L}(t_i)]}{\sqrt{2}[\sigma^2(R, t_i) - \sigma^2(R', t_i)]^{1/2}}\right\}. \quad \text{(A2)}$$

In the above equation, $\delta_{\rm c}(t, t_i) \simeq 1.686(1+z)/(1+z_i)$ is the critical excess density contrast needed at time t_i in order that the fluctuation collapses at time t; $\sigma(R, t_i) = \sigma(R)/(1+z_i)$ is the density contrast at the scale of the small clumps; $\delta_{\rm L}(t_i)$ is the initial density contrast of the (overdense) background region in which the clumps are embedded, and $\sigma(R', t_i)$ is the variance at the scale R' of the background region. Quite clearly, this formula reduces to the one in the text when the effect of the background region is ignored. Using the fact that the density contrasts scale as $1/(1+z)$ we can write

$$\frac{[\delta_{\rm c}(t, t_i) - \delta_{\rm L}(t_i)]}{\sqrt{2}[\sigma^2(R, t_i) - \sigma^2(R', t_i)]^{1/2}} = \frac{(1.686 - q)(1+z)}{\sqrt{2}[\sigma^2(R) - \sigma^2(R')]^{1/2}}, \quad \text{(A3)}$$

where $q = \delta_{\rm L}(t_i)(1+z_i)/(1+z)$ and the σs at the two scales are evaluated at the present epoch.

The $f_{\rm coll}$ can now be computed once the values for R' and q are specified. The size of the background region relevant to our problem is determined by the smoothing scale l from $R' = 1.77l(1+z)$ (see the discussion preceding equation 26). For q, we adopt two different values: (i) if we consider protocondensates that are turning around at the redshift of observation, $q \simeq 1.06$; (ii) for typical regions of size R', we can take $q \simeq \sigma(R')/(1+z)$. To make sure that we understand the effects of background adequately, we studied both these choices for q, although the first choice is physically more relevant.

We give in Table A1 the results for $f_{\rm coll}$ computed in the above manner for various cases.

Table A1. The effect of background on the collapsed fractions at various z.

z	$l(1+z)$	f_{coll}		
		$b = 1, case(i)$	$b = 1, case(ii)$	$b = 1.5, case(i)$
1.33	10.0	0.126	0.240	0.186
3.34	10.0	0.227	0.421	–
3.34	8.0	0.229	0.416	0.332
3.34	6.0	0.234	0.410	–
5.1	10.0	0.303	0.461	0.401
8.47	16.58	0.403	0.343	–

Comparing the values of $f_{\rm coll}$ in Table A1 with those of Table 1, we can arrive at the following conclusions. The specific numerical value of $f_{\rm coll}$ depends on the assumptions made regarding the background density. Since the characteristic mass scale that goes non-linear in an overdense region is larger than that in a typical region, the peak of $f_{\rm coll}$ occurs at a higher z then the corresponding redshifts in Table 1. This has the effect of decreasing $f_{\rm coll}$ at lower z. The effect is less significant at higher z. However, the numerical value differs from that calculated in the text by at most a factor of 2.

The results derived in the main text depend essentially on the combination $f_{tot} = f_N f_b f_{coll}$. The uncertainty in f_{tot} arising from $f_N f_b$ can easily be a factor of 2. Also note that in calculating f_{coll} we are integrating the mass function between fixed limits (M_1, M_2). As discussed in the text (see the paragraph after Table 1), this ignores the possible survival of H I in the objects of mass $M > M_2$ formed by the merging of smaller masses that have already cooled. This could also introduce an uncertainty in f_{tot} of about a factor of 2. Hence the effect of the background is likely to be subordinate to the other uncertainties. It must also be mentioned that, since f_{tot} appears in the expressions for S as an overall multiplicative constant, our results can be easily scaled for different values of f_{tot}.